Stem Cell Reports
Report
ISSCR
OPEN ACCESS

Heterogeneous Expression of SDF1 Retains Actively Proliferating Neural Progenitors in the Capillary Compartment of the Niche

Chang Zhu,[1] Swetha Mahesula,[1] Sally Temple,[2,*] and Erzsebet Kokovay[1,*]
[1]Department of Cell Systems and Anatomy, University of Texas Health Science Center at San Antonio, San Antonio, TX 78229, USA
[2]Neural Stem Cell Institute, Rensselaer, NY 12144, USA
*Correspondence: sallytemple@neuralsci.org (S.T.), kokovaye@uthscsa.edu (E.K.)
https://doi.org/10.1016/j.stemcr.2018.11.022

SUMMARY

The vascular compartment of the adult brain ventricular-subventricular zone (V-SVZ) is a critical regulator of neural stem cell and progenitor function. Blood enters the V-SVZ via arteries and arterioles to capillaries that then connect with venules and veins to return blood to the heart. We found that stromal cell-derived factor 1 (SDF1) is expressed by a subpopulation of V-SVZ vessels, the capillaries, and that actively proliferating neural stem cells (NSCs) and progenitors are preferentially associated with these SDF1-positive vessels. In contrast, slowly dividing or quiescent NSCs are most prevalent near SDF1-negative vessels. By conditional knockout, we found that loss of SDF1 signaling in NSCs stimulates lineage progression and NSC displacement from the vessel niche. With aging, SDF1/CXCR4 signaling is dysregulated, coincident with reduced proliferation and increased displacement of dividing cells from the vasculature. Our findings demonstrate SDF1-based vascular heterogeneity in the niche and suggest that reduced SDF1 signaling contributes to age-related declines in adult neurogenesis.

INTRODUCTION

The niche plays a critical role in regulating stem cell behavior, influencing quiescence, activation, and fate. In the adult murine brain, neural stem cells (NSCs) and their progeny lie in a large germinal zone, the ventricular-subventricular zone (V-SVZ), which lines the lateral ventricles. The V-SVZ has two major niche compartments: the apical ependymal layer, which faces the ventricle, and the vascular plexus on the striatal side (Figure 1A). NSCs, which are mostly quiescent, are clustered near the ependymal compartment, and send one fine apical process through the ependymal layer to contact cerebrospinal fluid in the lateral ventricle. NSCs also project a basal process that touches the V-SVZ vasculature (Mirzadeh et al., 2008; Shen et al., 2008; Tavazoie et al., 2008). Thus, by spanning from the ventricle to the V-SVZ vascular plexus, NSCs could be influenced by factors in both these compartments.

Upon activation, NSCs divide and give rise to transient amplifying cells (TACs) that expand the progenitor pool and generate neuroblasts. These neuroblasts migrate out of the niche migrate into the olfactory bulb, where they mature into neurons (reviewed in Kokovay et al., 2008). Proliferating NSCs and TACs are located adjacent to the V-SVZ vascular plexus (Shen et al., 2008; Tavazoie et al., 2008). Vascular endothelial cells can support self-renewal and neuronal fate choice in isolated NSCs from the developing and adult brain (Shen et al., 2004). However, not all V-SVZ vessels are contacted by proliferating NSCs and progenitors, raising the possibility that the vasculature is heterogeneous and that only some blood vessels promote and sustain NSC proliferation.

We previously determined that the chemokine stromal-derived factor 1 (SDF1), also called CXCL12, is essential for transplanted adult V-SVZ neural progenitor cells (NPCs) (which include NSCs and other classes of neural progenitors in the niche) to home to the V-SVZ vascular plexus. NPCs treated with SDF1 upregulate epidermal growth factor receptor and the laminin-binding molecule integrin-α6, suggesting that SDF1 could influence both the activation state and the binding of NPCs to the vasculature (Kokovay et al., 2010). However, how SDF1 signaling influences endogenous NSC and progenitor function is not known. Here we report that SDF1 is expressed in a subpopulation of blood vessels in the V-SVZ, corresponding to capillaries. We found that proliferating NSCs and progenitors are preferentially associated with the SDF1-positive capillaries; more quiescent, label-retaining NSCs were preferentially associated with SDF1-negative vessels. Conditionally deleting the CXCR4 receptor from NSCs and progenitors resulted in an early increase in NSC proliferation and numbers of TACs, suggesting that loss of CXCR4 stimulated the transition from NSCs to TACs. However, longer-term ablation reduced proliferation and resulted in fewer activated NSCs and TACs, indicating that NSCs and progenitors were depleted. Lastly, we determined that SDF1/CXCR4 signaling is reduced in the aging V-SVZ concomitant with reduced cell proliferation. Hence, impaired SDF1/CXCR4 signaling in the aging niche may contribute to age-associated declines in neurogenesis.

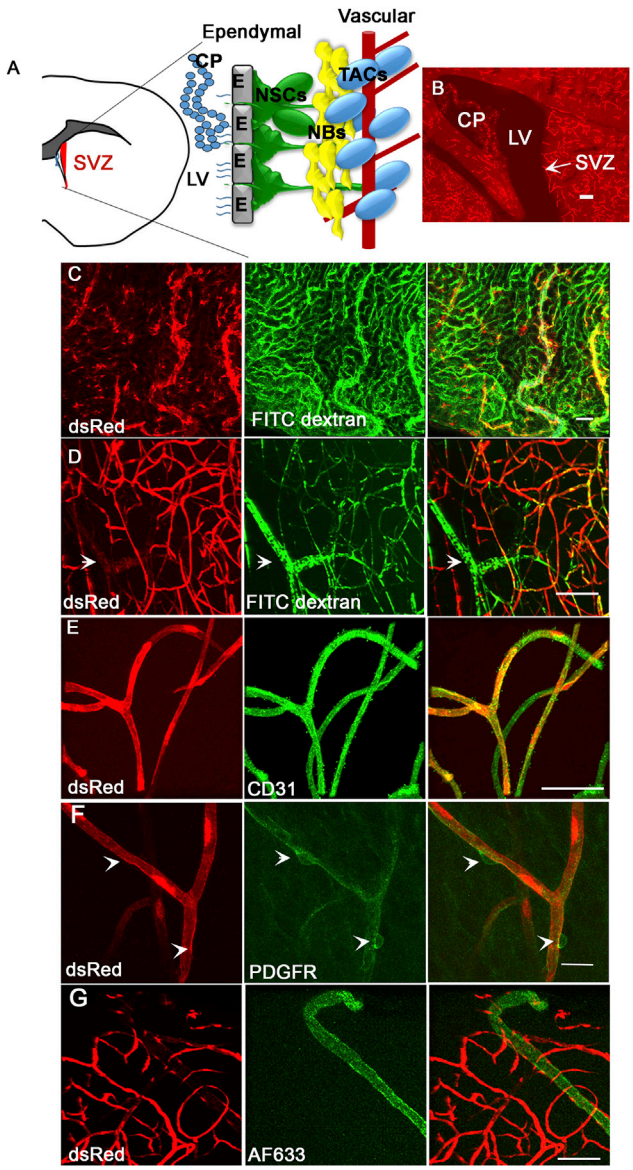

Figure 1. SDF1 Is Expressed by a Subset of Endothelial Cells in the V-SVZ

(A) Location of the SVZ and the different elements of the niche.

(B) Low magnification of a sagittal section from an *Sdf1*/DsRed mouse.

(C) DsRed is expressed by FITC dextran-positive and -negative cells in the choroid plexus.

(D) In the V-SVZ, *Sdf1* is expressed by the vasculature.

(E) DsRed is expressed by CD31-positive endothelial cells.

(F) DsRed is not expressed in pericytes.

(G) DsRed is not expressed by Alexa Fluor 633-positive arterioles. CP, choroid plexus; NBs, neuroblasts; LV, lateral ventricle; NSC, neural stem cell; TACs, transit amplifying cells. Scale bar, 50 μm. See also Figure S1.

RESULTS

SDF1 Is Heterogeneously Expressed by Vascular Cells in the V-SVZ

We characterized the expression of *Sdf1* in the adult V-SVZ niche (Figure 1A) using 8- to 12-week-old *Sdf1*DsRed transgenic mice that express fluorescent DsRed from the *Sdf1* promoter. *Sdf1* expression was strongest in the choroid plexus and brain vasculature (Figure 1B). To better define this expression in relation to the V-SVZ niche, we gave *Sdf1*DsRed mice a tail vein injection of fluorescein isothiocyanate (FITC)-labeled dextran to label blood vessels. We then dissected out the choroid plexus and V-SVZ whole mount. *Sdf1* was expressed in the choroid plexus in the vasculature and epithelial cells (Figure 1C). In the V-SVZ whole mounts, *Sdf1* was expressed in the vasculature (Figure 1D), which we confirmed by staining for laminin expressed by blood vessels (Figure S1A). *Sdf1* was expressed by $CD31^+$ vascular endothelial cells (Figure 1E), but not $PDGF\beta R^+$ pericytes (Figure 1F).

A subset of V-SVZ blood vessels did not express DsRed (arrow in Figure 1D). After injecting Alexa Fluor 633 hydrazide, which specifically stains arteries and arterioles (Kunisaki et al., 2013), into the tail vein of *Sdf1*DsRed mice, DsRed was not present on V-SVZ arterioles (Figure 1G), which we confirmed by co-staining for the arteriole marker smooth muscle actin (Figure S1B). Capillaries in the murine brain are 4–10 μm in diameter, whereas venules and arterioles are 10–100 μm in diameter (Macdonald et al., 2010). DsRed-positive vessels had a diameter of 5.08 ± 0.4249 μm and DsRed-negative vessels had an average diameter of 16.78 ± 1.93 μm, confirming that *Sdf1* is expressed by capillaries in the V-SVZ. All capillaries we measured were DsRed-positive and although some capillaries had low patches of expression, we did not observe any that did not express DsRed.

Proliferating Cells Are Associated with the SDF1-Expressing Capillaries

We and others have shown that proliferating NSCs and TACs are preferentially positioned adjacent to the V-SVZ vascular plexus (Shen et al., 2008; Tavazoie et al., 2008). To determine the relationship of these progenitor cells to SDF1-positive vessels, we administered a single injection of 5-ethynyl-2′-deoxyuridine (EdU) to *Sdf1*DsRed mice to label proliferating cells and euthanized them 2 hr later. Three-dimensional imaging of dissected V-SVZ whole mounts was analyzed using Imarus software. Proliferating cells were significantly more frequently associated with DsRed-positive than DsRed-negative vessels, with most proliferating cells either in

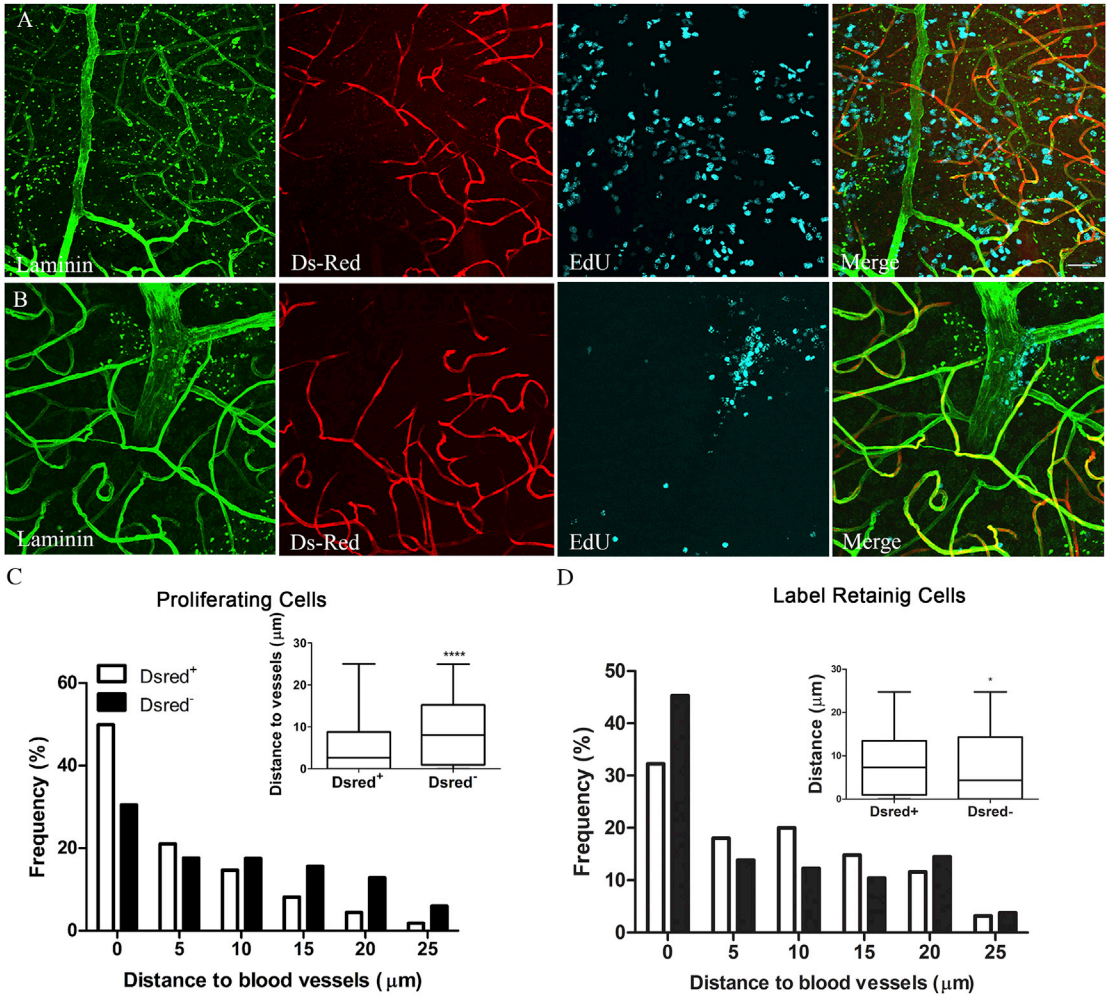

Figure 2. Proliferating NSCs Are Preferentially Associated with SDF1-Positive Vasculature

(A) Representative images showing proliferating cells (cyan) in relation to SDF1-positive (red) or SDF1-negative (green) vasculature. Scale bar, 100 μm (applies also to B).

(B) Same as in (A) except that label-retaining cells are labeled by cyan.

(C) Histogram with box-and-whisker plot inset showing the distribution of proliferative cells to DsRed^{+} and DsRed^{-} vasculature. n = 5,793 cells for DsRed^{+} and n = 2,854 cells for DsRed^{-}, measured in 4 mice per group. ****p < 0.0001 by Mann-Whitney test.

(D) Histogram with box-and-whisker plot inset showing the distribution of label-retaining cells to DsRed $^{+}$ and DsRed^{-}. n = 953 cells for DsRed^{+} and n = 653 cells for DsRed^{-}, measured in 6 mice per group. *p = 0.0105 by Mann-Whitney-test.

direct contact (0 μm away) or within 5 μm but not contacting the nearest DsRed-positive vessels (Figures 2A and 2C).

To analyze the relationships of quiescent or slowly dividing NSCs to these different vessels, we gave *Sdf1*DsRed mice daily injections of EdU for 5 days and euthanized them 2 weeks after the last injection to give differentiating cells time to leave the niche and highly proliferative cells time to dilute away the EdU label through repeated divisions. Slowly dividing cells were preferentially associated with DsRed-negative vasculature (Figures 2B and 2D).

Targeted Deletion of CXCR4 in Adult NPCs Stimulates Lineage Progression

To determine which population of V-SVZ cells expresses CXCR4, we used fluorescence-activated cell sorting (FACS) to separate activated NSCs, TACs, and neuroblasts as previously described (Santos et al., 2016). qRT-PCR for *Cxcr4* revealed that C*xcr4* is expressed by all three classes of NPCs. It was highly expressed by activated NSCs and TACs and to a lesser extent by neuroblasts (Figure 3A). To investigate the role of SDF1 signaling in V-SVZ NSCs, we generated Nestin-CreERT2CXCR4fl/flTdtomato mice (referred to as *Cxcr4*$^{fl/fl}$ mice) whereby tamoxifen induces

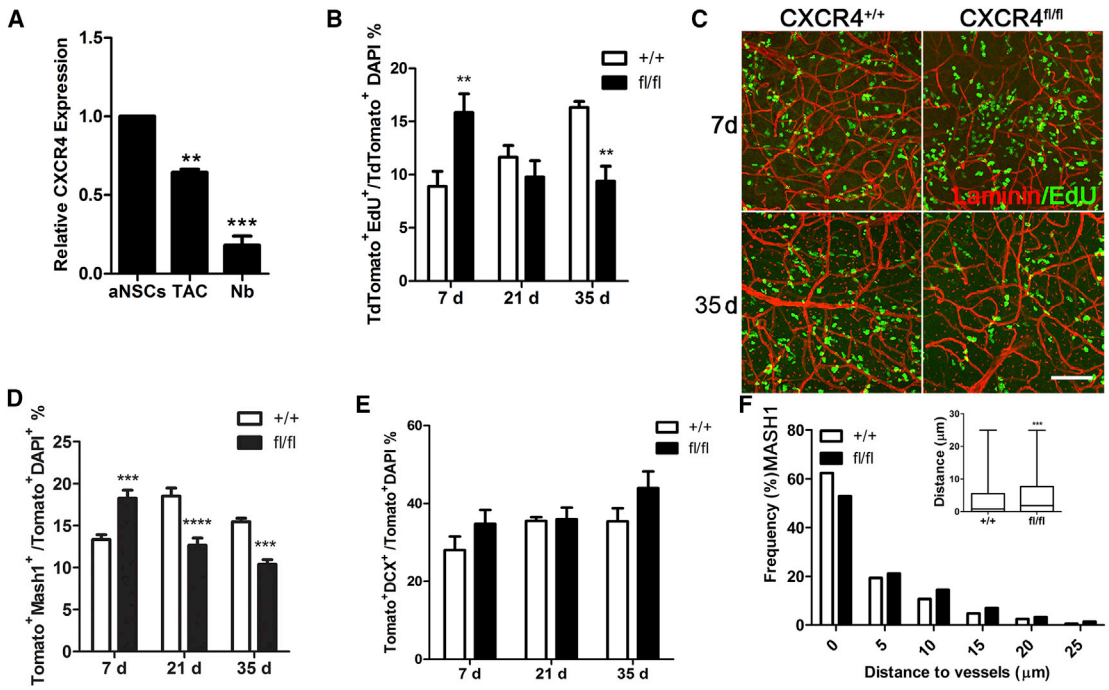

Figure 3. *Cxcr4* Knockdown Results in Lineage Progression and a Shift Away from the Vasculature

(A) CXCR4 expression in FACS-sorted lineage cells from the V-SVZ. **p < 0.01, ***p < 0.001.

(B) Percentage of EdU + TdTomato cells in V-SVZ whole mounts at 7, 21, and 35 days after tamoxifen injection (n = 4–5 mice/group; **p < 0.01 by two-way analysis of variance).

(C) Confocal images of whole mounts immunostained for laminin to label vasculature and EdU to label actively proliferating cells at 7 and 35 days after recombination. Scale bar, 100 μm.

(D) Percentage of MASH1+ TdTomato cells in V-SVZ whole mounts at 7, 21, and 35 days after tamoxifen injection (n = 3–5 mice/group; ***p < 0.001, ****p < 0.0001 by two-way analysis of variance).

(E) Numbers of TdTomato-positive neuroblasts did not significantly differ at any time point measured.

(F) *Cxcr4* deletion significantly shifted distance of MASH1 relative to the vasculature (n = 3,642 cells across 4 $Cxcr4^{+/+}$ mice, n = 3,166 cells across 3 $Cxcr4^{fl/fl}$ mice; p < 0.001 by Mann-Whitney test).

See also Figure S2.

nuclear localization of Cre to excise an exon of the *Cxcr4* gene and turn on the TdTomato label in Nestin$^+$ progenitor cells. After induction, we sorted TdTomato$^+$ cells from V-SVZ and confirmed that *Cxcr4* expression was reduced by qRT-PCR (67% ± 5% reduction in fl/fl mice versus controls; p = 0.0055). Recombination and reduced expression was confirmed using PCR to detect the excised exon and immunohistochemistry (Figure S2).

In a separate cohort of mice, we investigated the impact of CXCR4 loss on cell proliferation by injecting EdU to label dividing cells in three different groups at 7, 21, and 35 days after the last tamoxifen injection, sacrificing the mice 2 hr later. V-SVZ whole mounts were then dissected and immunostained with Mash1, a marker of activated type B and TACs (Codega et al., 2014; Kim et al., 2011) or neuroblast marker doublecortin (DCX). Using confocal microscopy combined with 3D image analysis, we analyzed the percentage of TdTomato$^+$ cells that were proliferating, detected by EdU labeling, and how this changed over time after *Cxcr4* deletion (Figures 3B and 3C).

The percentage of TdTomato-positive cells proliferating in Nestin-$Cxcr4^{fl/fl}$ mice was significantly increased compared with $Cxcr4^{+/+}$ mice 7 days after tamoxifen treatment. By 21 days after the last tamoxifen treatment, there was no significant difference in proliferation between groups. However, 35 days after tamoxifen treatment, proliferation in the $Cxcr4^{fl/fl}$ mice was reduced compared with controls. Numbers of MASH1-positive NSCs and TACs were significantly increased compared with controls in the V-SVZ at 7 days after *Cxcr4* deletion in the NSC lineage, then significantly reduced at 21 and 35 days (Figure 3D). In contrast, numbers of DCX-positive cells in the NSC lineage (indicating neuroblast identity) did not significantly change over time (Figure 3E).

Given our observation that dividing V-SVZ cells were most frequently associated with *Sdf1*DsRed-positive blood

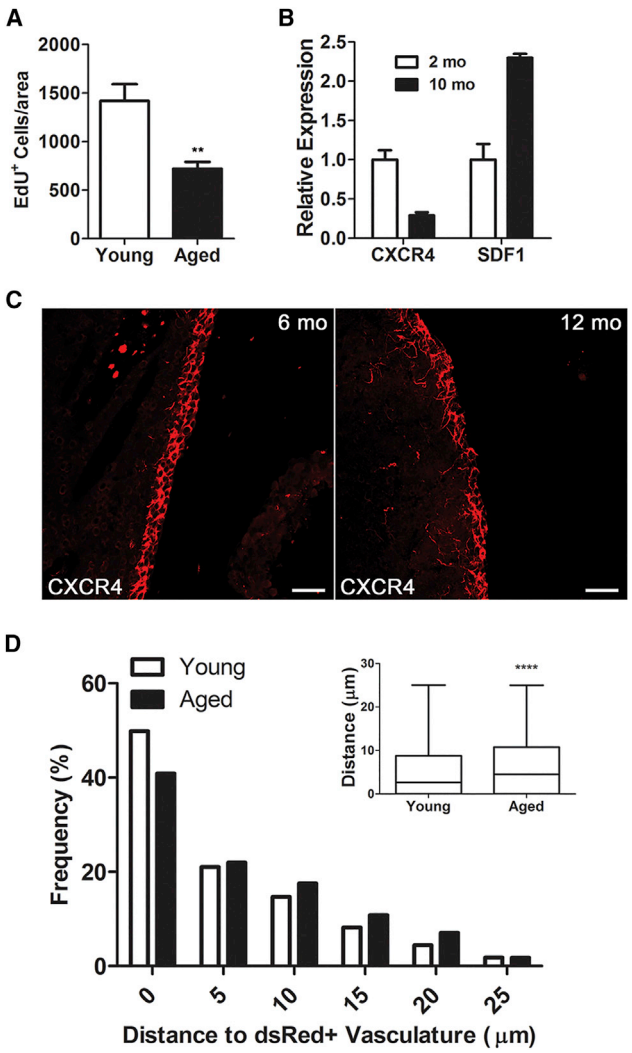

Figure 4. CXCR4/SDF1 Signaling Is Dysregulated in the Aging V-SVZ

(A) Numbers of EdU-positive cells in V-SVZ whole mounts in 2-month-old and 12-month-old mice (n = 4; **p < 0.01 by Student's t test).

(B) qRT-PCR analysis of *Cxcr4* and *Sdf1* expression in the V-SVZ of young and aged mice (n = 4/group).

(C) Representative confocal images of CXCR4 immunohistochemistry in coronal sections of the V-SVZ in 2-month-old and 12-month-old mice. Scale bars, 50 μm.

(D) Distribution of proliferating cells relative to *Sdf1*DsRed-positive vasculature. n = 5,793 cells for young mice, n = 2,208 cells for aged mice measured in 4 mice (****p < 0.001 by Mann-Whitney test).

vessels, we investigated whether conditional *Cxcr4* deletion in NSCs affected the position of proliferating cells relative to the vessel surface. *Cxcr4* deletion resulted in a small but significant shift of TACs away from the vasculature compared with controls (Figure 3F). The average distance of MASH1-positive cells from the vasculature increased in the $Cxcr4^{fl/fl}$ mice (5.09 ± 0.1617 μm, n = 3) compared with $Cxcr4^{+/+}$ mice (3.713 ± 0.075 μm, n = 3) at 14 days after tamoxifen treatment.

Reduced SDF1/CXCR4 Signaling between NSCs and the Vasculature with Age

Aging is associated with reduced V-SVZ NSC proliferation in 10- to 12-month-old mice (Bouab et al., 2011; Conover and Shook, 2011; Luo et al., 2008); however, the mechanisms underlying age-associated dysfunction are not clear. We confirmed in V-SVZ whole mounts that NSC and progenitor is reduced in aged mice (12-month-old mice) compared with young mice (2-month-old mice) (Figure 4A). *Cxcr4* expression was reduced in 10-month-old mice (29% ± 0.04%) compared with young mice, and *Sdf1* expression was increased by 30% ± 0.05% in aged mice (Figure 4B).

To confirm these results at the protein level, we performed immunohistochemistry for CXCR4 on coronal sections of mouse forebrain. CXR4 receptors were reduced in 12-month- old mice compared with 2-month-old mice (Figure 4C). To test whether this change was accompanied by changes in the distribution of proliferating cells relative to the vasculature, we gave *Sdf1*DsRed mice a single 2-hr pulse of EdU; distribution of cells was then compared in 2- and 12-month-old mice. Proliferating cells were significantly further from the vasculature in aged mice compared with controls (Figure 4D), similar to our results in $Cxcr4^{fl/fl}$ mice.

DISCUSSION

The vascular niche has been recognized as an important regulator of NSC function for over a decade. However, understanding of the signals that regulate NSC behavior is still limited. Prior studies have demonstrated a key role for SDF1 released from the SVZ plexus vasculature in the regulation of NSC lineage positioning and progression (Kokovay et al., 2010). Given that the SVZ plexus includes a variety of vessel types, we asked whether all or a subpopulation are important in this context. We found that capillaries express SDF1 while arterioles and venules are SDF1 negative, indicating a previously unappreciated heterogeneity in localized production of this important cytokine from the vascular niche. Moreover, proliferating cells were more frequently associated with SDF1-expressing cells, providing an explanation for prior observations that dividing cells are localized to some vessels, but not others (Shen et al., 2008; Tavazoie et al., 2008). The preferential localization of dividing V-SVZ cells near capillaries is intriguing. Indeed, brain capillaries are more permeable than venules and arterioles, which allows more efficient diffusion of nutrients and oxygen from the blood. SDF1

expression by capillaries may attract proliferating progenitors to meet the high metabolic demand of proliferating cells. Furthermore, the vasculature contributes to NSC proliferation (Gomez-Gaviro et al., 2012; Shen et al., 2008; Tavazoie et al., 2008) and quiescence (Delgado et al., 2014; Ottone et al., 2014); this paradox has limited our understanding of how the vasculature contributes to NSC behavior. Our finding that quiescent NSCs are associated with SDF1-negative vasculature suggests that this heterogeneity in vasculature might explain its opposing role in NSC activation states.

Here we report that *Cxcr4* was most highly expressed by activated NSCs and TACs. Loss of *Cxcr4* resulted in a transient increase and then reduced proliferation and numbers of activated NSCs and TACs. These findings suggest that loss of the CXCR4 receptor causes activated NSCs to differentiate into the more proliferative TACs, which may explain the early increase in proliferation we observed. TACs in turn produce DCX^+ neuroblasts that eventually leave the niche and migrate out toward the olfactory bulbs. We did not detect a significant increase in DCX^+ neuroblasts 35 days after conditional *Cxcr4* deletion, although the number of neuroblasts did trend upward. Our results suggest that an increase might be seen over the longer term, albeit tempered by migration of neuroblasts out of the niche.

After conditional *Cxcr4* deletion, we observed that proliferating cells were significantly further away from the nearest blood vessel surface. Previously, we showed that proliferating NSCs associate with the niche vasculature via α6β1 integrin expressed on NSCs, which can bind to blood vessel laminin (Shen et al., 2008). We also demonstrated that SDF1 treatment of isolated V-SVZ NSCs upregulated integrin-α6 (Kokovay et al., 2010). Thus, knockdown of *Cxcr4* may reduce integrin-α6 expression on NSCs, which would be expected to weaken the NSC-vasculature interaction. In addition to SDF1, niche endothelial cells secrete both pigment epithelium-derived factor and β-cellulin, which promote NSC self-renewal and TAC proliferation, respectively (Gomez-Gaviro et al., 2012; Ramirez-Castillejo et al., 2006). A shift of NSCs away from the vasculature may disrupt these signals, contributing to the reduced proliferation we observed.

Maintenance of CXCR4/SDF1 signaling could be important to ensure longevity of NSCs by preventing aberrant lineage progression. In this context, we note that *Sdf1* expression was higher in the aged V-SVZ, seen in this study as an increase between 2 and 12 months of age and by transcriptome analysis between 2 and 22 months of age (Apostolopoulou et al., 2017). SDF1 is regulated by a number of factors including the proinflammatory cytokine interleukin-1β, which we previously found was increased in the aged V-SVZ niche (Solano Fonseca et al., 2016), which may in part explain *Sdf1*1 upregulation. While the levels of *Sdf1* increased with aging, we found that between 2 and 12 months CXCR4 levels were significantly reduced; therefore, SDF1 signaling in aging NSCs to 12 months is likely to be reduced despite increased SDF1 production. These age-related changes in SDF1/CXCR4 were accompanied by reduced proliferation and a shift in the distribution of proliferating cells away from the vasculature. The molecular mechanisms underlying age-dependent reduction in neurogenesis are not known. However, both loss of NSCs from the niche (Shook et al., 2012) and increased NSC quiescence (Bouab et al., 2011) have been implicated. Loss of SDF1/CXCR4 signaling could contribute to both these mechanisms. Based on our conditional deletion experiments, loss of signaling could stimulate NSCs to produce TACs and deplete activated NSCs, which together could increase the proportion of quiescent NSCs within the niche.

In addition to perturbations in SDF/CXCR4 signaling with aging, this cytokine signaling pathway is also engaged after brain injury (Cheng et al., 2017). For example, it is well characterized that following stroke, SDF1 is upregulated in the damaged tissue, which stimulates NSC proliferation and progenitor migration to the ischemic area where they participate in repair (Ohab et al., 2006; Robin et al., 2006; Thored et al., 2009). Interestingly, in the peri-infarct region progenitors affiliate with SDF1-positive blood vessels that are undergoing angiogenesis, creating a vascular niche outside of the V-SVZ (Ohab et al., 2006).

Future studies are needed to determine whether regulating SDF1/CXCR4 signaling in the context of aging or disease could be valuable—for example, whether it could help maintain NSCs more effectively in neurogenic zones throughout life. Since NSCs are important in post-ischemic repair in mice and aging is a major risk factor for stroke, restoring NSC function (including CXCR4 signaling) could be beneficial for brain repair in the elderly.

EXPERIMENTAL PROCEDURES

Animals

All animal care and experimental procedures were approved by the UTHSCSA Institutional Animal Care and Use Committee. The following mouse lines were purchased from The Jackson Laboratory (Bar Harbor, ME) and bred in our animal facility: *Cxcr4* flox/flox mice (stock no. 008767), Nestin-Cre/ERT2 transgenic mice (stock no. 016261), FVB/N-Tg (GFAP-GFP) (stock no. 003257), and TdTomato Ai14 Cre reporter mice (stock no. 007914). *Sdf1*-DsRed mice were provided by Dr. Sean J. Morrison (UT Southwestern, Dallas, TX, USA). To generate conditional *Cxcr4* knockout mice, we crossed *Cxcr4* flox/flox mice with Nestin-Cre/ERT2 transgenic mice and TdTomato Ai14 Cre mice to obtain littermate mutants and controls: Nestin-Cre/TdTomato/*Cxcr4*flox/flox and Nestin-Cre/TdTomato/$Cxcr4^{+/+}$.

Tamoxifen, EdU, and Vascular Dye Injections

Tamoxifen solution (30 mg/mL in 10% ethanol and 90% sunflower oil) was injected intraperitoneally (i.p.) at 8 weeks of age. Mice received 180 mg/kg i.p. tamoxifen daily for 5 days. They were then sacrificed 7, 21, or 35 days after the first tamoxifen injection. For EdU, mice received five daily i.p. injections at (50 mg/kg) and were sacrificed 14 days after the last EdU injection to mark the label-retaining cells. For proliferation assays, mice received one i.p. injection of 50 mg/kg EdU 2 hr before they were sacrificed. EdU visualization was performed using the Click-iT EdU Imaging Kit (Invitrogen) according to the manufacturer's protocol. For vascular labeling, mice received 10 mg/mL FITC Dextran 150 (TdB Consultancy) in PBS at a dose of 50 mg/kg intravenously (i.v.). Mice were sacrificed after 5 min to visualize vasculature. For visualization of arterioles, mice received a 5 mg/kg Alexa Fluor 633 (Life Technologies) in PBS i.v. and were sacrificed after 4 hr.

Immunohistochemistry

Mice were perfused with PBS followed by 4% paraformaldehyde in phosphate buffer. V-SVZ whole mounts were dissected and processed as previously described (Solano Fonseca et al., 2016). Primary antibodies are described in Supplemental Experimental Procedures. Secondary antibodies were used at 1:250 (Cy- or DyLight-conjugated, Jackson ImmunoResearch Laboratories) at room temperature for 1 hr.

Image Analysis

For image analysis, 850 × 1,275× 30-μm tiles of 6 z stacks 30 μm thick were taken from the anterior V-SVZ whole mount using a Zeiss 710 confocal microscope. Using Imaris software, a surface was created of the entire depth of the image to determine the volume of the z stack. The vasculature surfaces were created under "Background Subtraction" to maximize the accuracy of the reconstruction. EdU-positive nuclei were labeled with the "Spots" function. "Outside SurfaceObjects" was used to measure the distances of any object (such as the EdU spots) to the nearest vasculature wall. The surface threshold was maintained as a constant to compare values across images and animals. All data were normalized to the total volume of the z stack.

FACS

V-SVZ tissues from GFAP-GFP mice were dissected and processed separately. Tissue was minced with a scalpel and digested with papain (Worthington, 1,200 units per 5 mice) and DNase (Worthington, 60 μg per 5 mice) for 30 min at 37°C and dissociated into single cells. Cells were incubated in Alexa 647-conjugated EGF (Life Technologies, 1:200), and PSA-NCAM-PE-IgM (1:11, Miltenyi Biotec) as previously described (Santos et al., 2016). Cells were sorted on a BD FACSAria II cell sorter (BD Biosciences) using 13 psi pressure and a 100-μm nozzle aperture. Cells were collected in PBS. Gates were set manually by using wild-type mice without Alexa 647-conjugated epidermal growth factor and isotype PE-IgM.

RNA Isolation and qRT-PCR

After sorting, cells were immediately lysed in Cell Lysis II Buffer (Life Technologies). Total RNA was isolated with the Cells-to-cDNA II Kit (Life Technologies) according to the manufacturer's instructions. For qRT-PCR, all reactions were carried out in triplicate on 3 biological replicates with an ABI PRISM 7900 Sequence Detection System using SYBR Green with specific primers. Data were normalized to GAPDH expression and analyzed by the 2-ΔΔCt method. The primers used were: *Gapdh* forward, 5′-AGG TCG GTG TGA ACG GAT TTG-3′, reverse 5′-TGT AGA CCA TGT AGT TGA GGT CA-3′; *Cxcr4* forward, 5′-AGC AGG TAG CAG TGA AAC CTC TGA-3′, reverse 5′-TGG TGG GCA GGA AGA TCC TAT TGA-3′.

Data Presentation and Statistics

Data are expressed as mean ± SEM. Mann-Whitney tests were used to determine statistical significance for distributions of distance measurements. Two-way ANOVAs were used for all serial knockout proliferation and differentiation analyses. Unpaired t tests or one-way ANOVAs were also used when appropriate. Significance levels were set at $p < 0.05$.

SUPPLEMENTAL INFORMATION

Supplemental Information includes Supplemental Experimental Procedures and two figures and can be found with this article online at https://doi.org/10.1016/j.stemcr.2018.11.022.

AUTHOR CONTRIBUTIONS

C.Z. performed the experiments. S.M. maintained and genotyped all mouse colonies. S.T. contributed funding and intellectually to the experimental design and interpretation and helped write the manuscript. E.K. contributed funding, contributed intellectually to the experimental design, helped interpret data, and wrote the manuscript.

ACKNOWLEDGMENTS

This work was supported by NIH-NIA R01 AG041861 and the William and Ella Owens Research Foundation. Data were generated in the Optical Imaging Core supported by UTHSCSA, NIH-NCI P30 CA54174 (CTRC at UTHSCSA), and NIH-NIA P01AG19316 and the Flow Cytometry Core, which supported by UTHSCSA, NIH-NCI P30 CA054174-20 (CTRC at UTHSCSA), and UL1 TR001120 (CTSA grant).

Received: July 23, 2018
Revised: November 29, 2018
Accepted: November 30, 2018
Published: December 27, 2018

REFERENCES

Apostolopoulou, M., Kiehl, T.R., Winter, M., Cardenas De La Hoz, E., Boles, N.C., Bjornsson, C.S., Zuloaga, K.L., Goderie, S.K., Wang, Y., Cohen, A.R., et al. (2017). Non-monotonic changes in progenitor cell behavior and gene expression during aging of the adult V-SVZ neural stem cell niche. Stem Cell Reports *9*, 1931–1947.

Bouab, M., Paliouras, G.N., Aumont, A., Forest-Berard, K., and Fernandes, K.J. (2011). Aging of the subventricular zone neural stem cell niche: evidence for quiescence-associated changes between early and mid-adulthood. Neuroscience *173*, 135–149.

Cheng, X., Wang, H., Zhang, X., Zhao, S., Zhou, Z., Mu, X., Zhao, C., and Teng, W. (2017). The role of SDF-1/CXCR4/CXCR7 in neuronal regeneration after cerebral ischemia. Front Neurosci. *11*, 590.

Codega, P., Silva-Vargas, V., Paul, A., Maldonado-Soto, A.R., Deleo, A.M., Pastrana, E., and Doetsch, F. (2014). Prospective identification and purification of quiescent adult neural stem cells from their in vivo niche. Neuron *82*, 545–559.

Conover, J.C., and Shook, B.A. (2011). Aging of the subventricular zone neural stem cell niche. Aging Dis. *2*, 49–63.

Delgado, A.C., Ferron, S.R., Vicente, D., Porlan, E., Perez-Villalba, A., Trujillo, C.M., D'Ocon, P., and Farinas, I. (2014). Endothelial NT-3 delivered by vasculature and CSF promotes quiescence of subependymal neural stem cells through nitric oxide induction. Neuron *83*, 572–585.

Gomez-Gaviro, M.V., Scott, C.E., Sesay, A.K., Matheu, A., Booth, S., Galichet, C., and Lovell-Badge, R. (2012). Betacellulin promotes cell proliferation in the neural stem cell niche and stimulates neurogenesis. Proc. Natl. Acad. Sci. U S A *109*, 1317–1322.

Kim, E.J., Ables, J.L., Dickel, L.K., Eisch, A.J., and Johnson, J.E. (2011). Ascl1 (Mash1) defines cells with long-term neurogenic potential in subgranular and subventricular zones in adult mouse brain. PLoS One *6*, e18472.

Kokovay, E., Shen, Q., and Temple, S. (2008). The incredible elastic brain: how neural stem cells expand our minds. Neuron *60*, 420–429.

Kokovay, E., Goderie, S., Wang, Y., Lotz, S., Lin, G., Sun, Y., Roysam, B., Shen, Q., and Temple, S. (2010). Adult SVZ lineage cells home to and leave the vascular niche via differential responses to SDF1/CXCR4 signaling. Cell Stem Cell *7*, 163–173.

Kunisaki, Y., Bruns, I., Scheiermann, C., Ahmed, J., Pinho, S., Zhang, D., Mizoguchi, T., Wei, Q., Lucas, D., Ito, K., et al. (2013). Arteriolar niches maintain haematopoietic stem cell quiescence. Nature *502*, 637–643.

Luo, J., Shook, B.A., Daniels, S.B., and Conover, J.C. (2008). Subventricular zone-mediated ependyma repair in the adult mammalian brain. J. Neurosci. *28*, 3804–3813.

Macdonald, J.A., Murugesan, N., and Pachter, J.S. (2010). Endothelial cell heterogeneity of blood-brain barrier gene expression along the cerebral microvasculature. J. Neurosci. Res. *88*, 1457–1474.

Mirzadeh, Z., Merkle, F.T., Soriano-Navarro, M., Garcia-Verdugo, J.M., and Alvarez-Buylla, A. (2008). Neural stem cells confer unique pinwheel architecture to the ventricular surface in neurogenic regions of the adult brain. Cell Stem Cell *3*, 265–278.

Ohab, J.J., Fleming, S., Blesch, A., and Carmichael, S.T. (2006). A neurovascular niche for neurogenesis after stroke. J. Neurosci. *26*, 13007–13016.

Ottone, C., Krusche, B., Whitby, A., Clements, M., Quadrato, G., Pitulescu, M.E., Adams, R.H., and Parrinello, S. (2014). Direct cell-cell contact with the vascular niche maintains quiescent neural stem cells. Nat. Cell Biol. *16*, 1045–1056.

Ramirez-Castillejo, C., Sanchez-Sanchez, F., Andreu-Agullo, C., Ferron, S.R., Aroca-Aguilar, J.D., Sanchez, P., Mira, H., Escribano, J., and Farinas, I. (2006). Pigment epithelium-derived factor is a niche signal for neural stem cell renewal. Nat. Neurosci. *9*, 331–339.

Robin, A.M., Zhang, Z.G., Wang, L., Zhang, R.L., Katakowski, M., Zhang, L., Wang, Y., Zhang, C., and Chopp, M. (2006). Stromal cell-derived factor 1alpha mediates neural progenitor cell motility after focal cerebral ischemia. J. Cereb. Blood Flow Metab. *26*, 125–134.

Santos, M.C., Tegge, A.N., Correa, B.R., Mahesula, S., Kohnke, L.Q., Qiao, M., Ferreira, M.A., Kokovay, E., and Penalva, L.O. (2016). miR-124, -128, and -137 orchestrate neural differentiation by acting on overlapping gene sets containing a highly connected transcription factor network. Stem Cells *34*, 220–232.

Shen, Q., Goderie, S.K., Jin, L., Karanth, N., Sun, Y., Abramova, N., Vincent, P., Pumiglia, K., and Temple, S. (2004). Endothelial cells stimulate self-renewal and expand neurogenesis of neural stem cells. Science *304*, 1338–1340.

Shen, Q., Wang, Y., Kokovay, E., Lin, G., Chuang, S.M., Goderie, S.K., Roysam, B., and Temple, S. (2008). Adult SVZ stem cells lie in a vascular niche: a quantitative analysis of niche cell-cell interactions. Cell Stem Cell *3*, 289–300.

Shook, B.A., Manz, D.H., Peters, J.J., Kang, S., and Conover, J.C. (2012). Spatiotemporal changes to the subventricular zone stem cell pool through aging. J. Neurosci. *32*, 6947–6956.

Solano Fonseca, R., Mahesula, S., Apple, D.M., Raghunathan, R., Dugan, A., Cardona, A., O'Connor, J., and Kokovay, E. (2016). Neurogenic niche microglia undergo positional remodeling and progressive activation contributing to age-associated reductions in neurogenesis. Stem Cells Dev. *25*, 542–555.

Tavazoie, M., Van der Veken, L., Silva-Vargas, V., Louissaint, M., Colonna, L., Zaidi, B., Garcia-Verdugo, J.M., and Doetsch, F. (2008). A specialized vascular niche for adult neural stem cells. Cell Stem Cell *3*, 279–288.

Thored, P., Heldmann, U., Gomes-Leal, W., Gisler, R., Darsalia, V., Taneera, J., Nygren, J.M., Jacobsen, S.E., Ekdahl, C.T., and Kokaia, Z. (2009). Long-term accumulation of microglia with proneurogenic phenotype concomitant with persistent neurogenesis in adult subventricular zone after stroke. Glia *57*, 835–849.

Stem Cell Reports, Volume *12*

Supplemental Information

Heterogeneous Expression of SDF1 Retains Actively Proliferating Neural Progenitors in the Capillary Compartment of the Niche

Chang Zhu, Swetha Mahesula, Sally Temple, and Erzsebet Kokovay

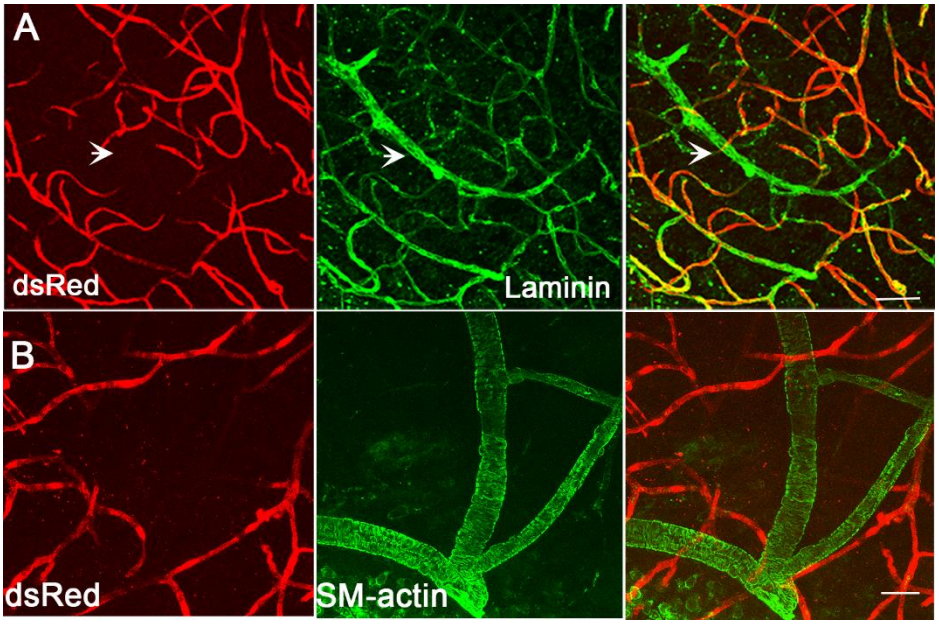

Supplemental Figure 1. Related to Figure 1. DsRed is expressed on a subset of the vasculature. (A) DsRed is absent from some blood vessels (arrow) immunostained for laminin. (B) DsRed is absent from smooth muscle actin positive arterioles. Scale bar = 50μm

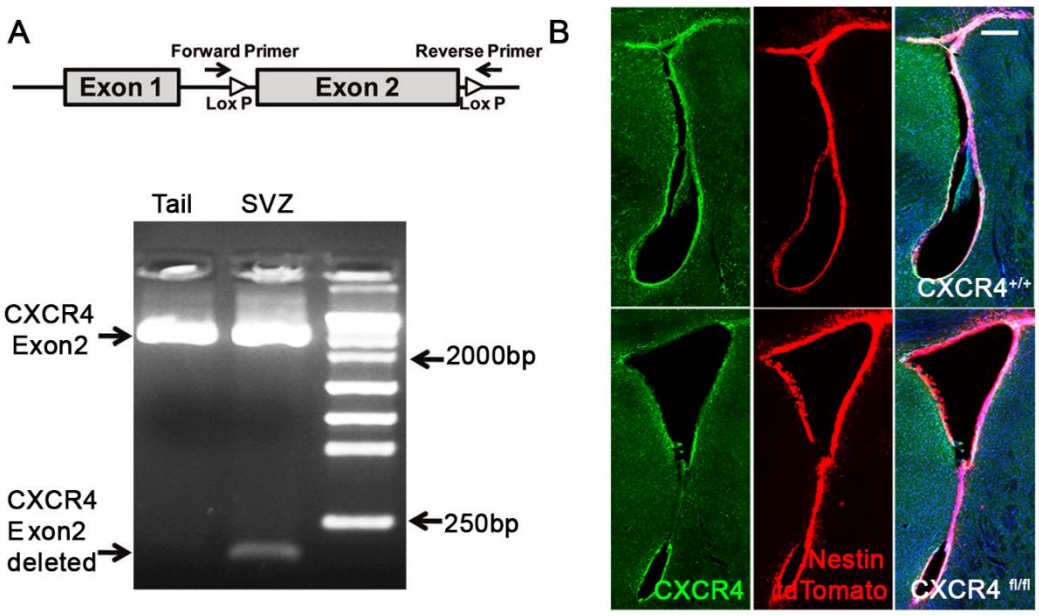

Supplemental Figure 2. Related to Figure 3. Tamoxifen injection results in excision of CXCR4 and reduced expression in NSCs. (A) Top panel: LoxP sites in the CXCR4 gene in the CXCR4fl/fl mice. Bottom panel: CXCR-deleted exon 2 is detectable after tamoxifen-induced recombination. (B) Immunohistochemistry for CXCR4 in the CXCR4fl/fl and CXCR4+/+ V-SVZ. Scale bar = 1000µm.

Supplemental Methods

Primary Antibodies for Immunohistochemistry

GFAP rabbit polyclonal (Dako, catalog #Z0334, RRID: AB_0013382, 1:500), goat anti-doublecortin (DCX, Santa Cruz Biotechnology, catalog #sc-8066, RRID:AB_2088494, 1:200), mouse anti-MASH1 (BD Pharmingen, catalog #556604, RRID:AB_396479, 1:100), rabbit anti-Laminin (Sigma, catalog #L9393, RRID: AB_477163, 1:500), rat anti-CD31 (BD Pharmingen, catalog # 550274, RRID: AB_393571, 1:100), rabbit anti-active Caspase-3 (Promega, catalog # G7481, RRID: AB_430875, 1:250) rat anti-PDGF Receptor beta (Abcam, catalog #ab91066, RRID: AB_10563302, 1:200) and rat anti-CXCR4 (1:25 R&D catalog # MAB21651).